On the Capacity of a Class of Acoustic Channels

Yashar Aval, Sarah Kate Wilson* and Milica Stojanovic

Northeastern University, Boston, MA, USA

*Santa Clara University, Santa Clara, CA, USA

Abstract

We consider a class of underwater acoustic communication channels where each propagation path can be characterized by a complex-valued Gaussian fading process. The capacity of such channels is computed and analyzed using three power allocation strategies: water-filling, uniform, and on-off uniform power allocation across the signal bandwidth. Our analysis considers the effects of imperfect channel estimation, delayed feedback, and pilot overhead, which contribute to about 1 bps/Hz loss from 4 bps/Hz at 20 dB SNR for the experimental channel. We find that given the long feedback delays associated with acoustic channels, all-on uniform power allocation which does not require feedback and is simple to implement emerges as a justified practical solution that outperforms the other strategies. Furthermore, when considering acoustic-specific propagation effects, such as frequency-dependent attenuation and colored noise, considerable gain can be achieved by selecting the frequency band according to the attenuation pattern and the available transmit power, e.g. at least 6 dB gain for a 10 km link when compared to transmission over a preselected frequency band of 10 kHz - 15 kHz.

Index Terms

Underwater acoustic communications, channel capacity, information rate, lower bound, Rician fading, water-filling, power allocation, OFDM.

I. Introduction

In contrast to radio communications, where capacity issues are well understood for point-to-point links (see e.g. [1], [2]), the fundamental question of acoustic channel capacity has been an elusive one, mainly because of the lack of well-established statistical channel models. Early work by Kwon and Birdsall [3], and Leinhos [4], which addressed the theoretical aspects, was followed by Kilfoyle et al. who performed the first experimental analyses [5], [6]. More recently, Radosevic et al. [7], [8], and Socheleau et al. [9] have focused on a Rician channel model supported by experimental measurements.

Approaching the Shannon channel capacity requires three elements: adaptive power allocation (spectrum shaping), adaptive modulation, and forward error correction (FEC) coding. The effects of power allocation and adaptive modulation on uncoded bit error rate (BER) have been analyzed for underwater acoustic channels in [10], where it was shown that adaptive modulation plays a critical role in achieving a desired BER, and adaptive power allocation reduces the required transmit power noticeably. An alternative, or additional approach is the use of adaptive FEC coding, which was shown in [11] to be effective in cases when only the SNR information is fed back to adjust the code rate, while the power and modulation level are kept constant across the carriers.

In this paper, we focus on calculating the ergodic and outage channel capacity, emphasizing the theoretically achievable rate rather than FEC coding.[1] We show that when considering the short-term channel variations, there is very little difference between water-filling and uniform power distribution in terms of the achievable rate.

Our present work has four objectives. First, we wish to re-visit the fundamental question of acoustic channel capacity and the rate achievable when the channel is not known but only estimated/predicted at the receiver/transmitter. We do so within the framework of orthogonal frequency-division multiplexing (OFDM). We perform two types of analysis, one based on the experimental data collected during the 2010 mobile acoustic communications experiment

[1]Given the limitation on the length of codewords, there will be a sacrifice on the achievable rate (e.g. see [12] for bounds on applicable code rates when codeword length is limited).

(MACE'10), and another based on a recently developed statistical channel model [13], where each propagation path is described as a non-zero-mean, first-order auto-regressive complex-Gaussian random process. Second, we investigate different power allocation strategies based on short-term fading statistics, including (i) water-filling; (ii) on-off power allocation [14], [15], where power is allocated in equal amounts but only to those carriers whose SNR is above the water-filling threshold, and (iii) uniform power allocation, where power is allocated equally to all subcarriers. Third, we address the issue of imperfect channel knowledge in light of (a) pilot overhead needed to estimate the channel at the receiver and the associated channel estimation errors, and (b) fundamental propagation delay that affects feedback, limiting the transmitter to operate only with outdated channel estimates. Finally, we consider acoustic-specific propagation with frequency-dependent attenuation and colored noise. In this case, we introduce two new power allocation strategies: water-filling based on the attenuation-and-noise profile only, and uniform power allocation, but across a favorable frequency band only. Unlike the case of short-term fading statistics, judicious power allocation based on acoustic propagation effects can increase the data rate and is robust in the presence of delay and channel estimation errors. Our results reflect the actual throughput after taking the guard intervals and pilot overhead into account.

The paper is organized as follows. In Sec. II we formally define the power allocation strategies, their respective capacities, and the corresponding lower bounds on the mutual information rate achievable in the presence of channel estimation errors (to which we shortly refer as "rate"). In Sec. III we discuss channel estimation and feedback strategies, and the impact of delay. We extend the findings to channels with frequency-dependent attenuation in Sec. III-C. Sec. IV is devoted to numerical results that quantify the achievable rate for the considered class of acoustic channels. Conclusions are summarized in Sec. V.

II. Achievable Rate

We consider a channel with M receiver elements described by the instantaneous transfer functions $H^1(f), \ldots, H^M(f)$, whose values at carrier frequencies $f_k = f_0 + k\Delta f, k =$

$0,\ldots,K-1$ are denoted by $H_k^m = H^m(f_k)$ and assumed to be constant over a subband of width $\Delta f = 1/T$. Defining the vector of channel responses, $\mathbf{H}_k = \left[H^1(f)\ \ldots\ H^M(f)\right]^T$, the signal received on the k-th carrier frequency is modeled as

$$\mathbf{y}_k = \sqrt{P_k}\mathbf{H}_k d_k + \mathbf{z}_k \tag{1}$$

where P_k is the power allocated to the k-th carrier, d_k is the unit-variance information symbol transmitted on this carrier, and $\mathbf{z}_k$ is zero-mean, circularly symmetric Gaussian noise of variance $\sigma^2_{z_k}$ for each receiver element. The noise is assumed to be independent across the receiver elements.[2] The total power allocated to the system is P_{tot}, and the total bandwidth is $B = K\Delta f$.

The capacity of this system is given by (see [2] for details)

$$C = \Delta f \sum_{k=0}^{K-1} \log_2\left(1 + \frac{P_k\|\mathbf{H}_k\|^2}{\sigma^2_{z_k}}\right)\ \text{[bps]} \tag{2}$$

where $\|.\|$ denotes the L_2 norm of a vector. Note that this capacity results from maximum ratio combining (MRC) at the receiver. Alternatively, the capacity can be expressed as C/B in bps/Hz.

The power allocation policy which maximizes the capacity is specified by the water-filling rule,

$$P_k = \left\{\begin{array}{l} \nu - \frac{\sigma^2_{z_k}}{\|\mathbf{H}_k\|^2},\ \text{when}\ \|\mathbf{H}_k\|^2 > \frac{\sigma^2_{z_k}}{\nu} \\ 0,\ \text{otherwise} \end{array}\right\},\ k = 0,\ldots K-1 \tag{3}$$

where the parameter ν is determined such that

$$\sum_{k=0}^{K-1} P_k = P_{tot} \tag{4}$$

The power allocation used here requires both the transmitter and the receiver to know the channel. In practice, estimates $\hat{\mathbf{H}}_k$ can be formed at the receiver and passed back to the transmitter, where they are used to implement a power allocation policy. We will consider two such policies: one based on water-filling, and another based on an *ad hoc* “on-off” rule. In both

[2]If the receiver elements are too closely spaced, such that the noise is correlated with some correlation matrix $\mathbf{R}_N$, we can whiten it by pre-multiplying by the received signal with $\mathbf{R}_N^{-1/2}$.

cases, channel estimation is accomplished using known pilot symbols, for which K_p carriers are reserved in advance. The remaining $K - K_p$ carriers are used for data (information), and indexed by the set $\mathcal{K}_d$. Setting aside a fraction α of the total power for the pilots, $(1-\alpha)P_{tot}$ is left for distribution across the data carriers. The two power allocation policies are specified below.

1) Imperfect water-filling: Power is allocated to the data carriers according to the rule (3), but with channel estimates $\hat{\mathbf{H}}_k$ replacing the unknown values $\mathbf{H}_k$:

$$P_k = \begin{cases} \nu - \frac{\sigma^2_{z_k}}{\|\hat{\mathbf{H}}_k\|^2}, \text{ when } \|\hat{\mathbf{H}}_k\|^2 > \frac{\sigma^2_{z_k}}{\nu} \\ 0, \text{ otherwise} \end{cases}, \; k \in \mathcal{K}_d \tag{5}$$

and the water level ν is determined such that

$$\sum_{k \in \mathcal{K}_d} P_k = (1-\alpha)P_{tot} \tag{6}$$

Note that water-filling may render some carriers with no power. These are the carriers whose frequencies are not favored by the channel. We refer to them as “bad carriers,” while the remaining carriers that are used to send data are called “good carriers.”

2) On-off uniform power allocation: Using the value of ν found under the previous policy, the available power $(1 - \alpha)P_{tot}$ is allocated in *equal* amounts P_d to the good carriers, while nothing is given to the bad carriers [14], [15]:

$$P_k = \begin{cases} P_d, \text{ when } \|\hat{\mathbf{H}}_k\|^2 > \frac{\sigma^2_{z_k}}{\nu} \\ 0, \text{ otherwise} \end{cases}, \; k \in \mathcal{K}_d \tag{7}$$

The bit rate achievable when only the channel estimates are available can be gauged from the lower bound on mutual information [2],[3]

$$R = \frac{T}{T+T_g} \cdot \Delta f \sum_{k \in \mathcal{K}_d} \log_2 \left(1 + \frac{P_k \|\hat{\mathbf{H}}_k\|^2}{\sigma^2_{z_k} + P_k \sigma^2_{\Delta H_k}} \right) \tag{8}$$

where $\sigma^2_{\Delta H_k} = \sigma^2_{\Delta H_k^m} = E\{|\Delta H_k^m|^2\}$ is the variance of the channel estimation error $\Delta H_k^m = \hat{H}_k^m - H_k^m$ which is assumed to be the same across all receiver elements, and the factor $T/(T+T_g)$

[3] We will refer to this quantity shortly as “rate.”

accounts for the multipath guard time T_g inserted between successive blocks of K carriers. The above expression is valid when the channel estimation error is orthogonal to the estimate $\hat{\mathbf{H}}_k$, e.g. when the estimator is a minimum-mean-squared error (MMSE) estimator.

When the channel is randomly varying, so are the capacity C and the rate R. To account for different channel realizations, one can use the notion of average capacity $\bar{C} = E\{C\}$, or outage capacity $C_{P_{out}}$, which is defined for a given outage probability P_{out} through $P_{out} = P\{C \leq C_{P_{out}}\}$. Similar definitions apply to the average rate $\bar{R}$ and the outage rate $R_{P_{out}}$.

III. Channel Estimation and Delay

For time-varying channels, we distinguish between two effects of delay, one occurring at the receiver and another at the transmitter (outdated feedback). The first effect is present when the receiver does not compute a new channel estimate in every block, but uses one block's estimate to predict the channel for several blocks. This is done to reduce the total pilot overhead. Delayed feedback causes the transmitter's estimate (which is used to allocate the power) to be outdated even if the receiver conveys its instantaneous estimate. Propagation delay thus presents a fundamental limitation, and one expects it to play a dominant role in an acoustic channel due to the low propagation speed.

To specify the rate, let us denote by D_r the number of blocks over which the receiver makes channel predictions (we will assume that predictions are made to the left and to the right of a pilot block, so a total of $2D_r$ predictions are made for each pilot block), and let D_t be the number of blocks involved in the delayed feedback. At the receiver, a new estimate $\hat{\mathbf{H}}_k(n_0)$ is made at times $n_0 = D_r, 3D_r + 1$, etc., while the predictions $\breve{\mathbf{H}}_k(n_0 + l)$ are made in-between, for $l = -D_r, \ldots D_r$. Hence, $\breve{\mathbf{H}}_k(n_0) = \hat{\mathbf{H}}_k(n_0)$ and $\breve{\mathbf{H}}_k(n_0 \pm 1)$, etc., are derived from $\hat{\mathbf{H}}_k(n_0)$. The channel estimate $\hat{\mathbf{H}}_k(n_0)$ is also known to the transmitter, but with a delay. The power $P_k(n_0)$ received during the n_0-th block has thus been allocated based on $\hat{\mathbf{H}}_k(n_0 - D_t)$. Note that while the receiver calculates a new prediction for every block, the transmitter may or may not do the same, i.e. it can either perform MMSE prediction based on the most recent estimate available from feedback, or keep this estimate as is and use it for power allocation until the next one

TABLE I
TIME TABLE OF THE ACTUAL CHANNEL, RECEIVER ESTIMATES AND PREDICTED VALUES, AND FEEDBACK INFORMATION USED AT THE TRANSMITTER FOR POWER ALLOCATION.

time [OFDM blocks]	0	1	2	3	4	5	6	7	8
actual instantaneous channel	$\mathbf{H}_k(0)$	$\mathbf{H}_k(1)$	$\mathbf{H}_k(2)$	$\mathbf{H}_k(3)$	$\mathbf{H}_k(4)$	$\mathbf{H}_k(5)$	$\mathbf{H}_k(6)$	$\mathbf{H}_k(7)$	$\mathbf{H}_k(8)$
channel estimate from pilots	$\hat{\mathbf{H}}_k(0)$	-	-	$\hat{\mathbf{H}}_k(3)$	-	-	$\hat{\mathbf{H}}_k(6)$	-	-
channel estimate at the receiver ($D_r = 1$)	$\breve{\mathbf{H}}_k(0)$	$\breve{\mathbf{H}}_k(1)$	$\breve{\mathbf{H}}_k(2)$	$\breve{\mathbf{H}}_k(3)$	$\breve{\mathbf{H}}_k(4)$	$\breve{\mathbf{H}}_k(5)$	$\breve{\mathbf{H}}_k(6)$	$\breve{\mathbf{H}}_k(7)$	$\breve{\mathbf{H}}_k(8)$
channel estimate at the transmitter ($D_t = 4$)	-	-	-	-	$\hat{\mathbf{H}}_k(0)$	$\hat{\mathbf{H}}_k(0)$	$\hat{\mathbf{H}}_k(0)$	$\hat{\mathbf{H}}_k(3)$	$\hat{\mathbf{H}}_k(3)$

becomes available. When the feedback delay is long, MMSE prediction at the transmitter is not practical as the amplitude of the channel prediction will decay over time, putting the transmitter in an SNR-starved mode where all of the power is assigned to only a few carriers. Therefore, we focus here on the case where the transmitter simply assigns power based on the most recent feedback of the receiver's channel estimate, which does not change between the pilot blocks. Table I shows the timing for channel prediction at the transmitter and the receiver, reflecting our choice for power allocation at the transmitter.

Looking at a given frame of $2D_r + 1$ blocks, pilots are assigned to the middle block (n_0), while the remaining blocks use all the carriers for data. Channel mismatch is thus due to both the noise-induced estimation error made in the pilot block and the subsequent change in the channel. From (8), we now have

$$\underbrace{\tilde{R}(n)}_{n=n_0+l} = \frac{1}{T+T_g} \sum_{k\in\mathcal{K}_d(m)} \log_2\left(1 + \frac{P_k(n)\|\breve{\mathbf{H}}_k(n)\|^2}{\sigma_{z_k}^2 + P_k(n)\sigma_{\Delta H_k}^2(l)}\right) \tag{9}$$

where $\sigma_{\Delta H_k}^2(l) = E\{|H_k^m(n_0+l) - \breve{H}_k^m(n_0+l)|^2\}$, and the set $\mathcal{K}_d(l)$ is the set of data carriers, which equals $\mathcal{K}_d$ when $l = 0$, or all the carriers when $l \neq 0$. Averaged over $2D_r + 1$ OFDM blocks with a pilot block in the middle, the instantaneous rate is[4]

$$R(n_0) = \frac{1}{2D_r+1} \sum_{l=-D_r}^{D_r} \tilde{R}(n_0+l) \tag{10}$$

This rate is a random variable whose statistics indicate the corresponding outage rate $R_{P_{out}}$, or

[4]An additional loss factor should be included for half-duplex channels.

average rate $\bar{R} = E\{R(n_0)\}$, taken over multiple channel realizations.

A. Channel model

To assess the impact of delay on the achievable rate, time-evolution of the channel has to be modeled. We focus on a statistical channel model with P propagation paths where the p-th path of the m-th receiving element is characterized during the n-th block by a random gain $h_p^m(n)$ and delay $\tau_p^m(n)$. The corresponding transfer function is

$$H_k^m(n) = \frac{1}{\sqrt{A_k}} \sum_p h_p^m(n) e^{-j2\pi f_k \tau_p(n)} \tag{11}$$

where the factor A_k accounts for frequency-dependent attenuation due to energy spreading and absorption. For the moment, we will set $A_k = 1$. In Sec. III-C, however, we will consider wideband channels in which dependence on A_k will have a significant effect on the achievable rate.

The path gains within each receiver element are modeled as independent, first-order auto-regressive processes that obey the following model:

$$[h_p^m(n) - \bar{h}_p^m] = \rho_{p,m}[h_p^m(n-1) - \bar{h}_p^m] + \sqrt{(1-\rho_{p,m}^2)}\sigma_{p,m}\chi_p^m \tag{12}$$

where $\bar{h}_p^m = E\{h_p^m(n)\}$ is the mean value of the gain, the variance of the gain is $\sigma_{p,m}^2 = E\{|h_p^m(n) - \bar{h}_p^m|^2\}$, and $\chi_p^m \sim \mathcal{CN}(0,1)$ is the process noise which is uncorrelated with $h_p^m(n-1)$ as well as across m and p. We also assume a normalization of path gains h_p^m such that $\sum_p \left(|\bar{h}_p^m|^2 + \sigma_{p,m}^2\right) = 1$ for $m = 1, \ldots, M$. Path independence follows from the fact that reflection points at which scattering occurs are sufficiently far apart [13].[5]

The one-step correlation coefficient ρ_p^m is related to the Doppler spread B_p^m of the p-th path to the m-th receiver element via $\rho_p^m = e^{-\pi B_p^m (T+T_g)}$ [13]. Time-evolution of the path delays is modeled as

$$\tau_p^m(n) = \tau_p^m(n-1) - a_p^m \cdot (T + T_g) \tag{13}$$

[5]Path independence does not imply independence of equivalent sample-spaced taps (an assumption that is often made in the literature, e.g. [1]).

where a_p^m is the Doppler factor that captures motion-induced time scaling on the p-th path to the m-th receiver element. Depending on the particular circumstances, Doppler scaling factors can be treated as deterministic or random, time-invariant or time-varying, known or unknown. Here, we assume that the residual Doppler factors (after initial resampling) are unknown, independent across paths, and follow a Gaussian distribution. Such an assumption is supported by the fact that the deterministic Doppler scaling due to transmitter/receiver motion may be removed during initial frame synchronization by resampling the received signal, and the residual Doppler is mainly caused by the random variations in the medium.

B. Channel Estimation and Prediction

We assume that the receiver finds the MMSE channel estimate using pilot carriers, and predicts the channel for the OFDM blocks which do not contain pilots. The MMSE estimation error corresponding to the pilot block is

$$\sigma^2_{\Delta H_k}(0) = E\{|H_k^m(n_0)|^2\} - E\{H_k^m(n_0)\mathbf{x}_P^{mH}\}E\{\mathbf{x}_P^m\mathbf{x}_P^{mH}\}^{-1}E\{H_k^m(n_0)^*\mathbf{x}_P^m\} \tag{14}$$

where $\mathbf{x}_P^m$ is a vector containing the values $y_k^m(n_0)d_k^*(n_0)$ of the signals received on the pilot carriers, and $(.)^H$ denotes the Hermitian operator (conjugate transpose).

We assume equi-spaced carriers, each with equal power. We also assume an MMSE channel estimator. The resulting channel estimation error can be expressed as (see [16] for details)

$$\sigma^2_{\Delta H_k}(0) = \lambda\frac{L\sigma^2_{z_k}}{\alpha P_{tot}} \tag{15}$$

where $L = BT_{mp}$, T_{mp} is the multipath spread, and $\lambda < 1$ is a scaling constant [16].[6]

Given the channel model specified by Eqs. (12) and (13), if the Doppler factors a_p^m follow a zero-mean Gaussian distribution with variance ${\sigma_a}^2$ (same statistics across channel taps and receiver elements), and amplitudes fade at the same rate $\rho_p^m = \rho$, MMSE channel predictions at

[6]Depending on the channel estimation technique, the estimation error variance may be different, but it will be proportional to (15) regardless of the technique. For example, if the channel impulse response is sparse, the estimation noise can further be reduced to $\lambda\frac{J\sigma^2_{z_k}}{\alpha P_{tot}}$, where J is the number of active channel taps [16].

the receiver are made as (see Appendix)

$$\breve{\mathbf{H}}_k(n_0+l) = e^{-|l|\phi^2}(\rho^l(\hat{\mathbf{H}}_k(n_0) - \bar{\mathbf{H}}_k(n_0)) + \bar{\mathbf{H}}_k(n_0)) \tag{16}$$

where $\phi = \pi\sqrt{2}f_k(T+T_g)\sigma_a$, and $\bar{\mathbf{H}}_k(n_0)$ is a vector of length M, whose m-th element is $\bar{H}_k^m(n_0) = \frac{1}{\sqrt{A_k}}\sum_p \bar{h}_p^m e^{-j2\pi f_k \tau_p(n_0)}$. With equal noise power across carriers, this channel prediction contains an error whose variance is (see Appendix)

$$\sigma^2_{\Delta H_k}(l) = \rho^{2|l|}e^{-2l^2\phi^2}\sigma^2_{\Delta H_k}(0) + (1-e^{-2l^2\phi^2})\sum_p (\bar{h}_p^m)^2 + (1-\rho^{2|l|}e^{-2l^2\phi^2})\sum_p \sigma^2_{p,m} \tag{17}$$

The first term in the above expression reflects the noise-induced channel estimation error made in the pilot block, while the second and third terms reflect the prediction error caused by the channel dynamics.

The variance (17) can be substituted directly into the expressions (9) and (10) for the rate. The trade-off between the number of pilots and the channel estimation errors then becomes clear: as D_r increases, the total overhead decreases (K_p pilots cover $(K-K_p)+2D_rK$ data carriers), but every new channel prediction, made farther away from the pilot block, brings a stronger error.

C. *Frequency-dependent Attenuation*

In wideband underwater acoustic channels, frequency-dependent attenuation represents another source of frequency selectivity. Unlike the multipath, whose structure changes with the motion of the transmitter and receiver, nominal characteristics of the frequency-dependent attenuation and noise spectrum can be assessed a-priori. That knowledge can be used at the transmitter to perform spectrum shaping in a manner similar to water-filling [17].

The key difference between the multipath-induced frequency selectivity and the frequency-dependent large-scale attenuation is that the latter changes much more slowly. Referring to the channel model (11), the factor A_k can thus be regarded as a statistical parameter of the channel, and we shall consequently refer to the related spectrum shaping (for lack of a better term) as “statistical water-filling”. We also define a second strategy, analogous to uniform power allocation, where the power is allocated uniformly, but only over a limited bandwidth favored

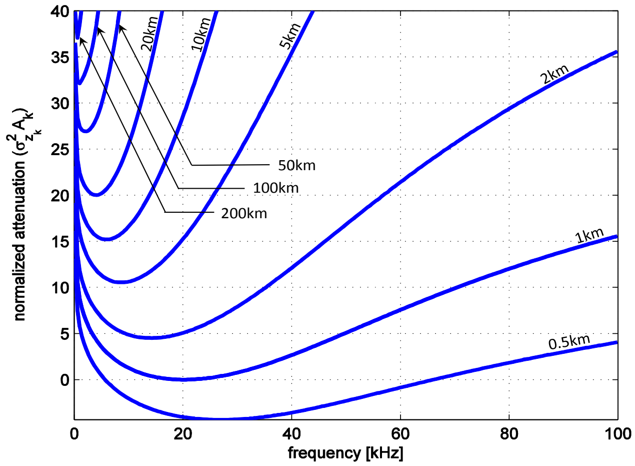

Fig. 1. The frequency-dependent attenuation-noise profile, $\sigma^2_{z_k}A_k$. Normalization is performed such that the 0 dB level corresponds to the minimum point at 1 km. The noise profile is generated as in [17] with the parameters set to no wind ($w = 0$) and moderate shipping activity ($s = 0.5$). The spreading is assumed to be spherical.

by the attenuation and noise profile. We refer to this strategy as band-limited uniform.

Given the parameters A_k and $\sigma^2_{z_k}$, which we assume to be the same for all receiving elements, statistical water-filling is applied as follows:

$$P_k = \begin{cases} \nu - \frac{\sigma^2_{z_k}A_k}{M}, \text{ when } \nu > \frac{\sigma^2_{z_k}A_k}{M} \\ 0, \text{ otherwise} \end{cases}, \quad k = 0, \dots K-1 \tag{18}$$

where water level ν is selected as before, according to (4) or (6).

The frequency band for band-limited uniform policy is selected using the value of ν from statistical water-filling to identify the carriers for which $\nu > \frac{\sigma^2_{z_k}A_k}{M}$. Power is allocated uniformly to those carriers, while nothing is given to the rest. Fig. 1 illustrates the relevant attenuation-noise characteristic, $\sigma^2_{z_k}A_k$.

IV. Results

Given the candidate power allocation policies, the question arises as to what performance can they deliver in terms of the rate, and how does this performance compare with the channel capacity. On the one hand, we have the imperfect water-filling which aspires to achieve the optimum (but ignores the penalty of channel estimation errors), while on the other hand we

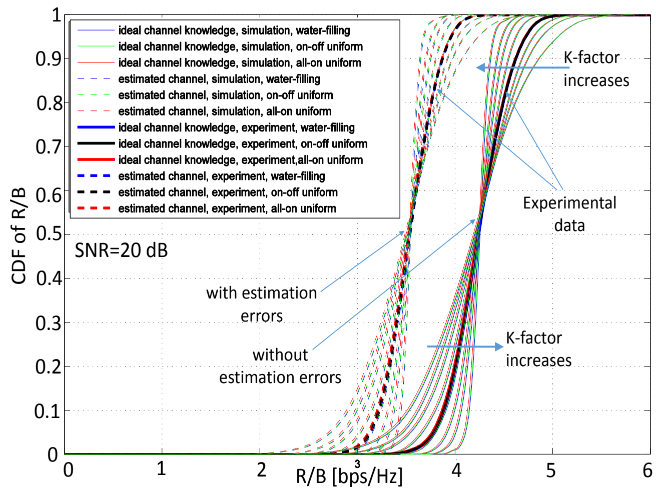

Fig. 2. Cumulative distribution function of the rate (8). The average K-factor takes values 0, 0.5, 1, 2, 4, 8 , 16, 64.

have on-off power allocation which does not follow any optimization incentive, but is simpler to implement and operate. Finally, we have the unknown-channel feedback-free policy in which power is allocated equally to all carriers.

The results presented below are obtained using simulation and experimental data. The experimental data were recorded in a 100 m deep, 3-7 km long mobile channel, with 256 carriers occupying 10 kHz - 15 kHz acoustic band (for details of deployment, see [18]). The results are based on 1664 OFDM blocks transmitted over a period of 3.5 hours. The guard interval is $T_g = 16$ ms and the block duration is $T = 51$ ms for both the experimental data and the simulation. The simulated channel follows the model of Sec. III-A, where the average path gains and path delays are selected according to the channel geometry that matches the experimental one.[7] We select 50 different channel responses (which vary slightly in the placement of transmitter and receiver) and add random time-variation over the duration of 100 OFDM blocks (5000 blocks in total). To describe the variation, we use the notion of the average Rician K-factor as introduced in [19], $\bar{K} = \sum_p (\bar{h}_p^m)^2 / \sum_p \sigma_{p,m}^2$, which is assumed to be the same for all receiver elements.

[7]The average multipath profile is characterized by the mean gain magnitudes, equal for all receiver elements, 1β, 0.9β, 0.5β, 0.45β, 0.4β, 0.3β, 0.1β and nominal delays 0, 0.4, 1.7, 3, 5.5, 7.6, 11.5 ms. The corresponding variances are 1γ, 0.2γ, 0.5γ, 0.15γ, 0.15γ, 0.07γ, 0.1γ, and the factors β and γ are selected such that the normalization $\sum_p (\bar{h}_p^m)^2 + \sum_p \sigma_{p,m}^2 = 1, m = 1, \ldots, M$ is satisfied and the desired average Rician K-factor, $\bar{K} = \sum_p (\bar{h}_p^m)^2 / \sum_p \sigma_{p,m}^2$, is achieved. Doppler scaling factors are generated independently for each path and receiver element as Gaussian distributed with zero mean and standard deviation σ_a which varies between 0 and 5×10^{-5}.

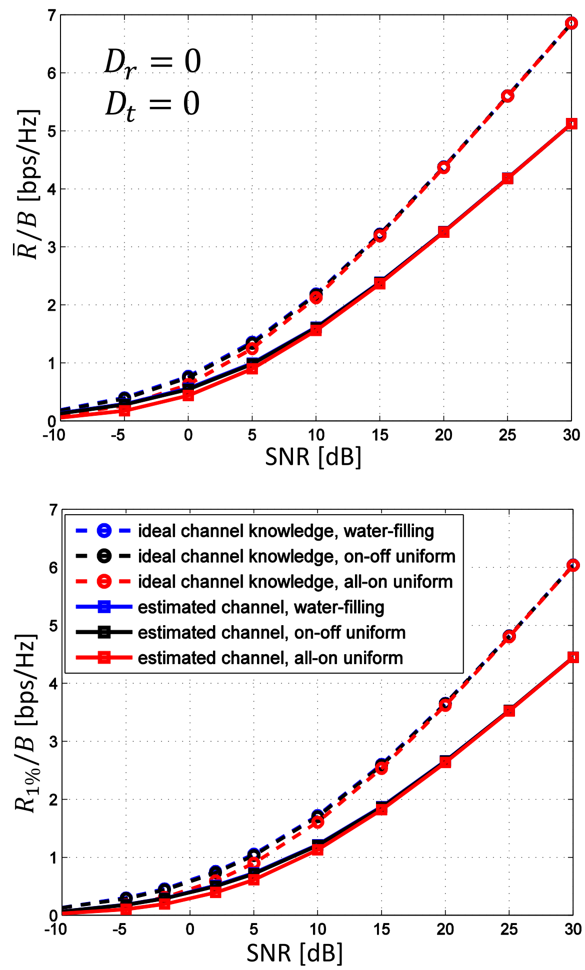

Fig. 3. Average rate (top) and 1% outage rate (bottom), calculated using experimental data for single-element receiver. This result corresponds to instantaneous feedback.

The results are based on $K_p = K/8$ channel estimation pilots and pilot power ratio, $\alpha = 1/8$, except for the genie-aided benchmark cases labeled "ideal channel knowledge," where no pilots are needed (data on all carriers).

Fig. 2 shows the cumulative distribution function of the rate (8) calculated using simulated, as well as experimentally measured channels. We note that the experimental channel matches closely with $\bar{K} = 2$. Different curves on this plot can be used to determine the outage rate for different $\bar{K}$.

Next, we compare the power allocation strategies in terms of the average rate $\bar{R}$ and and the

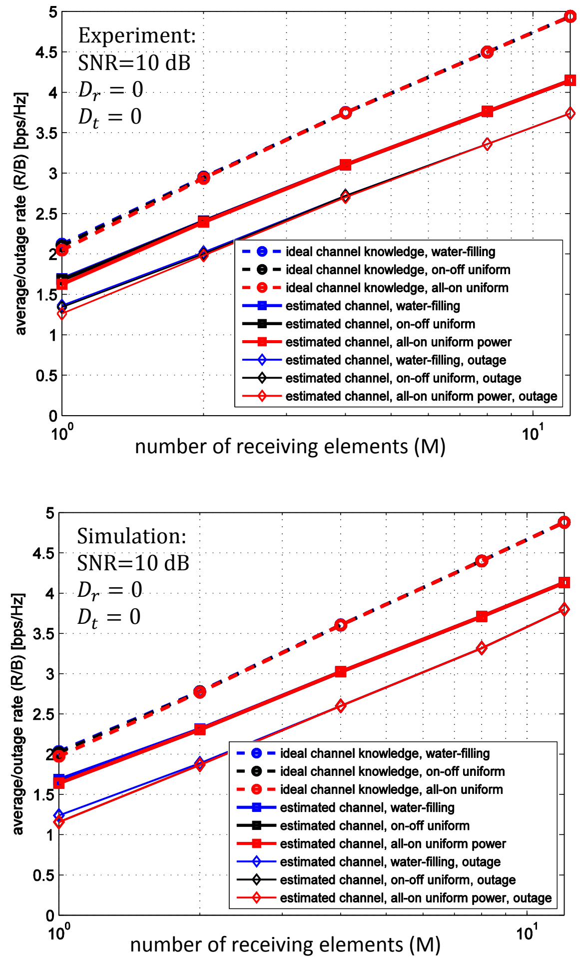

Fig. 4. Average rate calculated using experimental data (top) and simulation (bottom) vs. the number of receiving elements. This result illustrates the effect of noise-induced channel estimation errors, and the difference between average and outage rate. Pilots are inserted into every OFDM block, feedback is assumed to be instantaneous, and the average SNR is 10 dB for each receiver element.

outage rate $R_{P_{out}}$. Fig.3 shows $\bar{R}$ (top) and $R_{1\%}$ (bottom) vs. SNR, calculated from experimental data. Similar results are obtained in simulation. Different power allocation strategies are seen to perform with negligible difference on this channel, providing about 4 bps/Hz at the SNR of 20 dB under ideal channel knowledge. Channel estimation errors impact all the strategies in a very similar manner, causing a loss of about 1 bps/Hz at 20 dB SNR.

Fig. 4 extends these results to the case of multiple receiving elements for experimental (top) and synthetic data (bottom). The rate now increases linearly with the logarithm of the number of receiver elements, while the loss of rate due to channel estimation errors remains almost unchanged. Similarly, the difference between the average and the 1% outage rate remains at about 0.5 bps/Hz regardless of the number of receiver elements.

The benefits of water-filling and on-off uniform power allocation policies are investigated in Fig. 5 (top). This figure shows the increase in rate over that achieved by the uniform power allocation policy, $\Delta R/B = R/B - (R/B)_{all-on}$. The maximum gain of 0.15 bps/Hz (and 0.13 bps/Hz for on-off uniform) in the rate occurs at about 0 dB SNR for the single receiving element case ($M = 1$). The gain of water-filling and on-off uniform power allocation also decreases with multi-element combining, but eventually saturates as the aperture remains fixed and the signals received by different elements become correlated. To establish a benchmark, we compare this result to a hypothetical channel (bottom) whose transfer function for each receiver element follows an independent Rayleigh distribution over carriers, $P\{|H_k^m| = x\} = 2x\mathrm{e}^{-x^2}$ with $\sigma_{z_k} = 1/\mathrm{SNR}$. The M channels are assumed to be independent and MRC is applied at the receiver. The gain of water-filling for this hypothetical channel closely matches that of the experimental channel for up to four receiver elements, but beyond that, the results differ as the assumption of independence among receiver elements no longer holds for the experiment. Nevertheless, this observation corroborates the general conclusion that the frequency-domain channel coefficients may be modeled as Rayleigh distributed, and that MRC closes the performance gap between uniform power allocation and water-filling, even for SNR-starved channels with instantaneous feedback.

A. *The Impact of Feedback Delay*

The results of Figs. 3, 4 and 5 take into account only the imperfect channel knowledge at the receiver, i.e. they assume an instantaneous feedback. In the presence of feedback delay, the performance of all-on uniform allocation will be the same, while the other two strategies can only perform worse. This fact is illustrated in Fig. 6 (top). In the absence of feedback delay, water-filling and on-off policies offer a small advantage; however, the situation is equalized and eventually reversed with outdated feedback, as the “good” and “bad” carriers are no longer

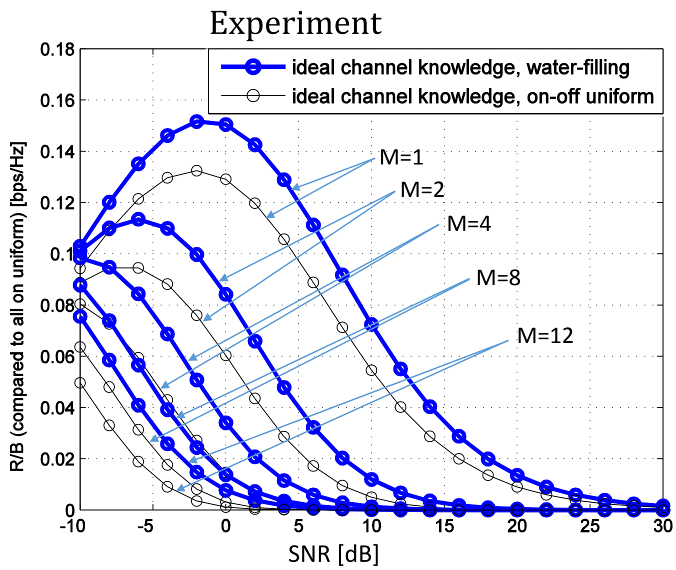

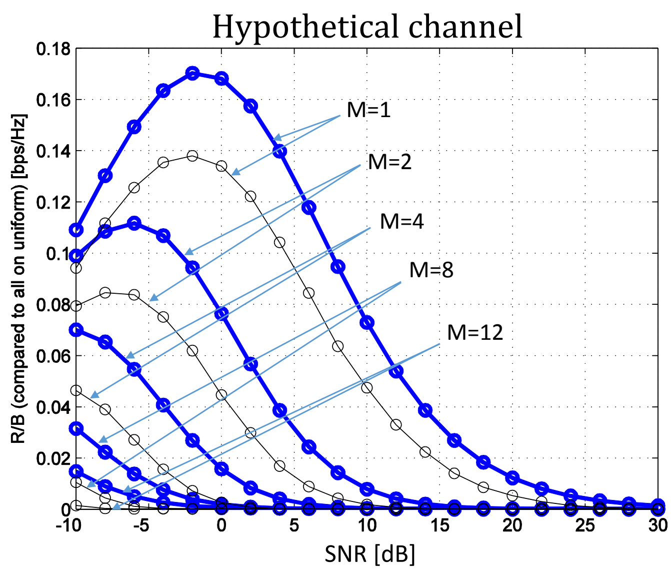

Fig. 5. Increase in the average rate of water-filling and on-off uniform power allocation policies over all-on policy. This result demonstrates the reduction in the benefits of water-filling when the SNR or the number of receiver elements are increased.

identified correctly. These facts speak strongly in favor of using the simple, feedback-free, all-on uniform power allocation.

The effect of receiver's prediction window $\pm D_r$ is illustrated in Fig. 6 (bottom). As D_r increases, the pilot overhead is reduced, but the penalty of prediction errors become significant (c.f. (17)), eventually reducing the average rate. Thus, there exists an optimal choice of D_r for a given channel (e.g. D_r=4 when ρ=0.99 and $\sigma_a = 0$).

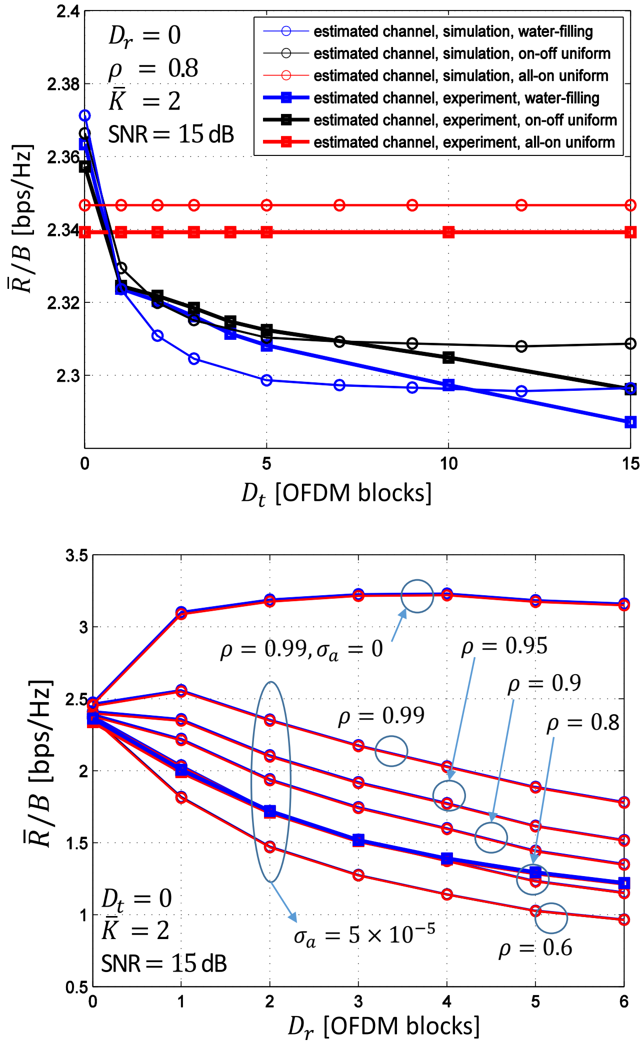

Fig. 6. Average rate as a function of feedback delay (top) and receiver's prediction window (bottom). Multiple values of the one-step correlation coefficient, ρ, and the standard deviation of the Doppler factor, σ_a, are used for simulation. These figures also include the results from the experimental channel.

Channel estimation plays a key role in the achievable rate (with uniform, or any other power allocation policy). In practice, the trade-off between accurate channel estimation and pilot overhead can additionally be negotiated by employing decision-directed tracking algorithms, whose implementation is much simplified under uniform power allocation.

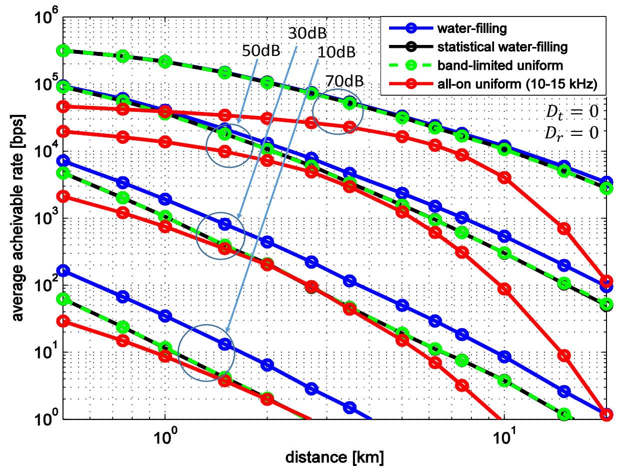

Fig. 7. Average rate vs. distance between the transmitter and the receiver for multiple values of transmit power (10 dB, 30 dB, 50 dB, and 70 dB), and four power allocation policies. Channel parameters (A_k and σ_{z_k}) are calculated from Fig. 1. Ideal channel knowledge is assumed both at the transmitter and the receiver, and the all-on uniform policy is applied across the frequency band 10 kHz - 15 kHz regardless of the distance and transmit power.

B. Frequency-dependent Attenuation

Figures 7 – 11 demonstrate the effect of frequency-dependent attenuation on the average rate. These results are based on normalized transmit power, where the 0 dB level corresponds to the power required to sustain an average SNR of 0 dB over a bandwidth of 1 Hz at the optimal carrier frequency and a distance of 1 km. Frequency-dependent channel parameters are calculated from Fig. 1. To establish a benchmark, we also include the all-on uniform policy, where power is assigned uniformly to all of the carriers within the frequency band 10 kHz - 15 kHz which is the same as the band used in the experiment.

Fig. 7 and 8 compare four power allocation policies as a function of distance, assuming ideal channel knowledge and instantaneous feedback. Water-filling provides the most significant gain at lower transmit powers (10 dB - 30 dB), doubling the rate compared to other methods. As the power increases (e.g. to 70 dB), all methods except the all-on uniform policy will eventually load all of the carriers within the favorable frequency range and therefore perform similarly. Fig. 9 shows a guideline for selecting the optimal frequency band for various distances and transmit powers.

While the results of Figs. 7 and 8 promote application of water-filling in SNR-starved channels,

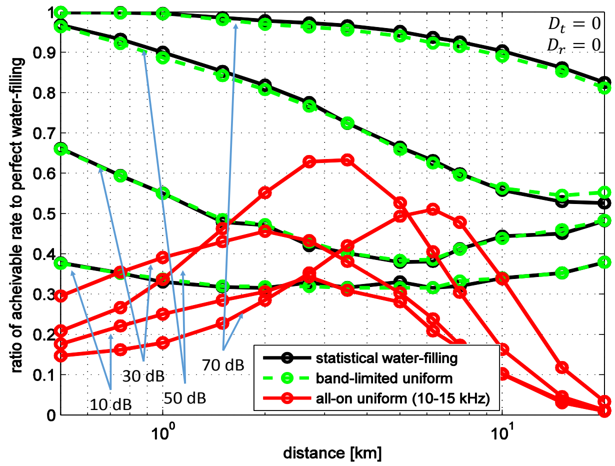

Fig. 8. Ratio of the average rate for statistical water-filling, band-limited uniform, and all-on uniform power allocation policies to water-filling, vs. the distance between the transmitter and the receiver. System parameters are the same as in Fig. 7, and ideal channel knowledge is assumed both at the receiver and the transmitter.

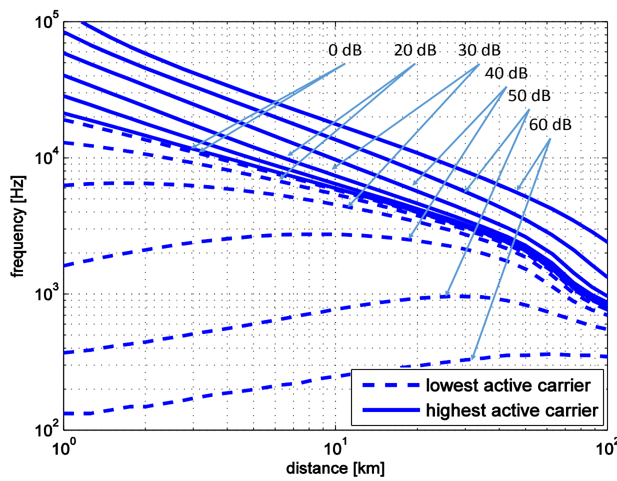

Fig. 9. Optimal frequency band vs. distance for different values of transmit power. Band-limiting is based on large-scale channel parameters and the transmitter frequency response is assumed to be flat.

they assume instantaneous feedback. Fig. 10 shows how the benefit of water-filling fades away with the introduction of feedback delay. For example, assuming a residual Doppler factor with standard deviation of $\sigma_a = 5 \times 10^{-5}$ (equivalent of motion at the speed of about 0.07 m/s) and one step correlation coefficient $\rho = 0.8$, and feedback delay as long as 20 OFDM blocks (which is equivalent to the round-trip propagation delay of a 1 km link), water-filling is outperformed by the other strategies. The performance of all-on uniform policy depends on the preselected

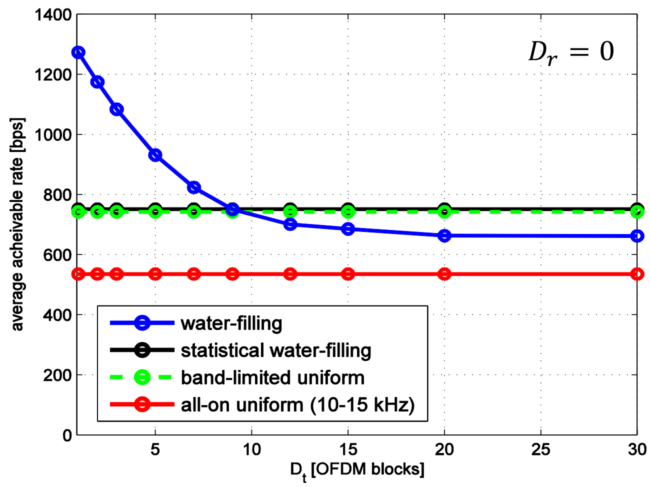

Fig. 10. Achievable rate vs. transmitter feedback delay for multiple power allocation policies. Distance between the transmitter and the receiver is 1 km, normalized transmit power is 30 dB, $\rho = 0.8$, and $\sigma_a = 5 \times 10^{-5}$. The receiver is assumed to have ideal channel knowledge while this knowledge (no noise-induced channel estimation error). The rest of the parameters are the same as Fig. 7.

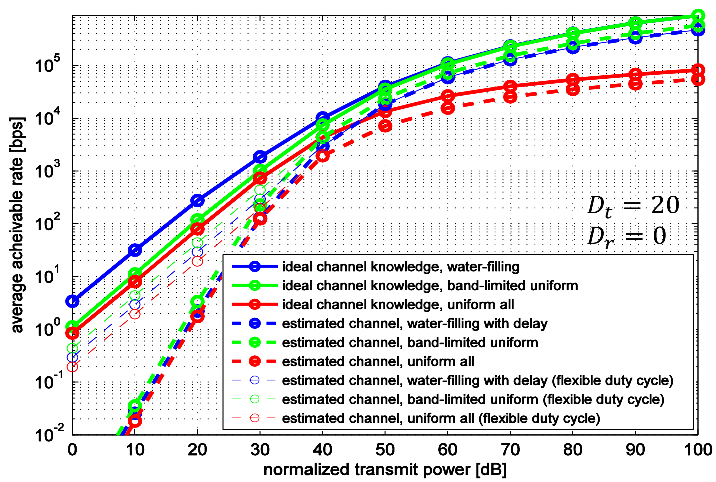

Fig. 11. Achievable rate vs. normalized transmit power for estimated channels compared to perfect channel knowledge (distance is 1 km). This figure compares the capacity of estimated channel to the ideal channel knowledge scenario, and also shows that allowing for a flexible duty cycle at the transmitter improves the channel capacity significantly at lower SNRs.

frequency band. For example, the frequency range between 10 kHz - 15 kHz is a good choice for a 3 km link if an achievable rate of no more than 10 kbps is desired, while it is far from optimal for higher transmit powers or longer distances.

.

Fig. 11 demonstrates the loss in performance due to channel estimation error in low SNR regime. One method of reducing the estimation error is to transmit at a higher power, gP_{tot} for $1/g$ of the time, where $g \geq 1$ is the gain factor. This transmission strategy keeps the average transmit power unchanged while allowing for a degree of freedom in optimizing the trade-off between the power consumption and the penalty of imperfect channel estimation. Fig. 11 shows that a flexible duty cycle can increase the capacity significantly for channels whose capacity is less than about 5 kbps (for the distance of 1 km).

V. Conclusion

A capacity analysis was presented for acoustic channels in which each path is modeled as an auto-regressive, non-zero-mean complex-Gaussian process. Numerical results, obtained via simulation and experimentally measured channels, indicate the average achievable rate (lower bound) on the order of 3 bps/Hz at the SNR of 20 dB (1% outage rate is lower by 0.5 bps/Hz) in the presence of channel estimation errors. This achievable rate increases almost linearly with the logarithm of the number of receiver elements. On comparing three power allocation policies – water-filling, on-off uniform and all-on uniform – the first two were found to offer little or no advantage on this channel. The simple, feedback-free policy which does not require any knowledge of the channel and allocates the power uniformly to all the carriers of an OFDM signal, thus emerges as a justified choice for practical implementation. Its throughput can be maximized by judicious pilot allocation across blocks to strikes a balance with the channel estimation accuracy which remains the priority of an acoustic receiver.

We also considered the frequency-dependent attenuation profile and colored noise, showing that while uniform power allocation remains the favorable choice, selecting the frequency band based on the channel parameters and available power becomes crucial for optimizing the rate. Future work will address long-term channel variation, and the attendant methods for rate maximization via power control.

Appendix

This appendix contains the derivation of MMSE channel prediction (Eq. (16)) and the associated prediction error variance (Eq. (17)) based on the channel model introduced by Eqs. (12)

and (13).

To find the MMSE channel prediction for l OFDM blocks into the future (or the past), we need the correlation between $H_k^m(n)$ and $H_k^m(n+l)$,

$$\begin{aligned} E\{H_k^{m*}(n)H_k^m(n+l)\} &= E\left\{\sum_p h_p^{m*}(n)e^{j2\pi f_k\tau_p^m(n)}\sum_q h_q^{m*}(n+l)e^{-j2\pi f_k\tau_q^m(n+l)}\right\} \\ &= \sum_p\sum_q E\left\{h_p^{m*}(n)h_q^m(n+l)\right\}E\left\{e^{j2\pi f_k(\tau_p^m(n)-\tau_q^m(n+l))}\right\} \end{aligned} \tag{19}$$

The first expected value in the above expression, $E\{h_p^{m*}(n)h_q^m(n+1)\}$, can be simplified as

$$E\{h_p^{m*}(n)h_q^m(n+l)\} = \bar{h}_p^{m*}\bar{h}_q^m + \rho^l\delta_{p,q}\sigma_{p,m}\sigma_{q,m} \tag{20}$$

and the second expected value, $E\{e^{j2\pi f_k(\tau_p^m(n)-\tau_q^m(n+l))}\}$ is assumed to be zero for $p \neq q$.[8] For $p = q$, this expected value is

$$\begin{aligned} E\{e^{j2\pi f_k(\tau_p^m(n)-\tau_p^m(n+l))}\} &= \int_{-\infty}^{\infty} e^{-j2\pi f_k a_p^m l(T+T_g)}\frac{1}{\sigma_a\sqrt{2\pi}}e^{-\frac{(a_p^m)^2}{2\sigma_a^2}}da_p^m \\ &= e^{-(\sqrt{2}\pi f_k l(T+T_g)\sigma_a)^2} \\ &= e^{-l^2\phi^2} \end{aligned} \tag{21}$$

where the Doppler factors, a_p^m, are modeled as independent across the paths and receiver elements, and follow a Gaussian distribution with variance σ_a^2 for all paths and receiver elements.

Substituting Eq. (20) and Eq. (21) into Eq. (19), we have

$$E\{H_k^{m*}(n)H_k^m(n+l)\} = e^{-l^2\phi^2}\sum_p(|\bar{h}_p^m|^2 + \rho^l\sigma_{p,m}^2) \tag{22}$$

where the correlation has two terms, one for the average path gains $\bar{h}_p^m$, and another for the randomly varying part of the path gains, $(h_p^m - \bar{h}_p^m)$, which has the variance of $\sigma_{p,m}^2$. These terms fade at rates $e^{-l^2\phi^2}$ and $\rho^l e^{-l^2\phi^2}$, respectively. The correlation (22) suggests the following

[8]This assumption holds true when the difference between the arrival times τ_p^m and τ_q^m is greater than T/K.

MMSE prediction,

$$\breve{H}_k^m(n+l) = e^{-l^2\phi^2}(\rho^l(\hat{H}_k^m(n) - \bar{H}_k^m(n)) + \bar{H}_k^m(n)) \tag{23}$$

which can be presented as Eq. (16) in vector form. It is straight-forward to show that this prediction satisfies the MMSE criteria.

The variance of the prediction error is,

$$\begin{aligned}
\sigma^2_{\Delta H_k^m}(l) &= E\{|\breve{H}_k^m(n+l) - H_k^m(n+l)|^2\} \\
&= \rho^{2|l|}e^{-2l^2\phi^2}E\{|\hat{H}_k^m(n) - H_k^m(n)|^2\} + (1-e^{-2l^2\phi^2})E\{|\bar{H}_k^m(n)|^2\} \\
&+ (1-\rho^{2|l|}e^{-2l^2\phi^2})E\{|H_k^m(n) - \bar{H}_k^m(n)|^2\} \\
&= \rho^{2|l|}e^{-2l^2\phi^2}\sigma^2_{\Delta H_k}(0) + (1-e^{-2l^2\phi^2})\sum_p(\bar{h}_p^m)^2 + (1-\rho^{2|l|}e^{-2l^2\phi^2})\sum_p \sigma^2_{p,m}
\end{aligned} \tag{24}$$

Note that since all the receiver elements are assumed to have the same statistics, the right-hand side of the above expression is not a function of m. Therefore, in the text we omit the superscript m in $\sigma^2_{\Delta H_k^m}(l)$ for simplicity.

Acknowledgments

This work was supported by the following grants: ONR N00014-09-1-0700, NSF CNS-1212999.

References

[1] Y. Yao and G. Giannakis, "Rate-maximizing power allocation in OFDM based on partial channel knowledge," *IEEE Trans on Wireless Comm.*, vol. 4, no. 3, May 2005.

[2] T. Yoo and A. Goldsmith, "Capacity and power allocation for fading MIMO channels with channel estimation error," *IEEE Trans. on Info. Theory*, vol. 52, no. 5, May 2006.

[3] H. Kwon and T. Birdsall, "Channel capacity in bits per Joule," *IEEE J. of Ocean. Eng.*, vol. 11, no. 1, Jan. 1986.

[4] H. Leinhos, "Capacity calculations for rapidly fading communications channels," *IEEE J. of Ocean. Eng.*, vol. 21, no. 2, Apr. 1996.

[5] D. Kilfoyle, J. Preisig, and A. Baggeroer, "Spatial modulation over partially coherent multiple-input/multiple-output channels," *IEEE Trans on Sig. Proc.*, vol. 51, no. 3, Mar. 2003.

[6] ——, “Spatial modulation experiments in the underwater acoustic channel,” *IEEE J. of Ocean. Eng.*, vol. 30, no. 2, Apr. 2005.

[7] A. Radosevic, D. Fertonani, T. Duman, J. Proakis, and M. Stojanovic, “Capacity of MIMO systems in shallow water acoustic channels,” in *44-th Asilomar Conf. on Sig., Sys. and Comp.*, Nov. 2010.

[8] ——, “Bounds on the information rate for sparse channels with long memory and i.u.d. inputs,” *IEEE Trans. on Comm.*, vol. 59, Dec. 2011.

[9] J.-M. Passerieux, F.-X. Socheleau, and C. Laot, “Achievable rates over doubly selective Rician-fading channels under peak-power constraint,” *IEEE Trans. on Wireless Comm.*, vol. 12, no. 2, Feb. 2013.

[10] A. Radosevic, R. Ahmed, T. Duman, J. Proakis, and M. Stojanovic, “Adaptive OFDM modulation for underwater acoustic communications: Design considerations and experimental results,” *IEEE J. of Ocean. Eng.*, vol. 39, no. 2, Apr. 2014.

[11] G. Lim, S. K. Willson, L. J. Cimini, and D. P. Taylor, “On higher order modulations for OFDM in frequency selective fading channels,” in *IEEE Comm. Letters*, Apr. 2013.

[12] Y. Polyanskiy, H. Poor, and S. Verdu, “Channel coding rate in the finite blocklength regime,” *IEEE Trans. on Info. Theory*, vol. 56, no. 5, May 2010.

[13] P. Qarabaqi and M. Stojanovic, “Statistical characterization and computationally efficient modeling of a class of underwater acoustic communication channels,” *IEEE J. of Ocean. Eng.*, vol. 38, no. 4, Oct. 2013.

[14] W. Yu and J. Cioffi, “Constant-power waterfilling: performance bound and low-complexity implementation,” *IEEE Trans. on Comm*, vol. 54, no. 1, Jan. 2006.

[15] S. K. Willson and M. Stojanovic, “When does unequal power-loading make sense?” in *2014 Info. Theory and App. Wrokshop (ITA)*, 2014.

[16] M. Morelli and U. Mengali, “A comparison of pilot-aided channel estimation methods for OFDM systems,” *IEEE Trans. on Sig. Proc.*, Dec. 2001.

[17] M. Stojanovic, “On the relationship between capacity and distance in an underwater acoustic communication channel,” in *ACM SIGMOBILE Mob. Comp. and Comm. Review (MC2R)*. New York, NY, USA: ACM, 2007.

[18] Y. M. Aval and M. Stojanovic, “Differentially coherent multichannel detection of acoustic OFDM signals,” *IEEE J. of Ocean. Eng.*, Jun. 2014.

[19] A. Radosevic, T. Duman, J. Proakis, and M. Stojanovic, “Selective decision directed channel estimation for OFDM communications over multipath Rician fading channels,” in *13th IEEE Int. Workshop on Sig. Proc. Adv. in Wireless Comm. (SPAWC)*, Jun. 2012.